Solid-State ^{23}Na Nuclear Magnetic Resonance of Sodium Complexes with Crown Ethers, Cryptands, and Naturally Occurring Antibiotic Ionophores: A Direct Probe to the Sodium-Binding Sites

Alan Wong and Gang Wu*

Department of Chemistry, Queen's University, Kingston, Ontario, Canada K7L 3N6

Received: June 12, 2000; In Final Form: August 24, 2000

We report a systematic solid-state ^{23}Na nuclear magnetic resonance study of sodium complexes with crown ethers, cryptands, and naturally occurring antibiotic ionophores. Precise information about ^{23}Na quadrupole coupling constants and chemical shifts was determined from analysis of ^{23}Na magic-angle spinning (MAS) NMR spectra. We found that the experimental ^{23}Na chemical shifts can be related to an empirical parameter that is a function of the atomic valence of the donor ligand, the Na^+−ligand distance, and the coordination number (CN) around the Na^+ ion of interest. A reasonably good correlation was also observed between the ^{23}Na quadrupole parameters measured in $CDCl_3$ solution and those measured in the solid state, indicating that the cation exchange is slow in $CDCl_3$. In MeOH solution, however, neither ^{23}Na quadrupole parameters nor chemical shifts of the Na−ionophore complexes show correlation with the corresponding solid-state data. Finally, we report the ^{23}Na chemical shift tensor in $Na(12C4)_2ClO_4$: $\delta_{11} = \delta_{22} = -1$ ppm and $\delta_{33} = -15$ ppm.

1. Introduction

Alkali metal elements are indispensable in many biological processes. Unlike divalent metal ions, monovalent alkali metal ions generally exhibit weak association to biological macromolecules. Their roles have been thought primarily to be as bulk electrolytes that stabilize surface charges on proteins and nucleic acids. However, recent discoveries have revealed that alkali metal ions also play unique structural roles in biological systems. For example, the presence of K^+ or Na^+ ions is critical in the formation of G-quartet structures in telomeric DNAs.[1−4] Cs^+ and K^+ ions are also found to promote pentameric assembly of DNA bearing the nonstandard nucleobase isoquanine.[5] K^+-specific binding sites in proteins and in ion channels have recently been characterized by X-ray crystallography.[6]

Among NMR active alkali metal nuclei, ^{23}Na is relatively easy to study because of its 100% natural abundance and relatively high magnetogyric ratio, $\gamma = 7.0761 \times 10^7$ rad·s^{-1}·T^{-1}. However, the fact that ^{23}Na is also a quadrupolar nucleus ($I = 3/2$ and $Q = 0.1 \times 10^{-28}$ m^2) imposes some practical difficulties not only on carrying out NMR experiments, but also on interpreting the experimental data. One of the major problems of solution ^{23}Na NMR is related to its intrinsically poor spectral resolution, arising from a combination of small chemical shift range and large line width due to efficient ^{23}Na quadrupole relaxation. In addition, the rapid cation exchange between free and bound states often prevents one from observing separate NMR signals for different cation-binding sites. In contrast, solid-state NMR spectra exhibit intrinsically high resolution due to relatively long relaxation times and restricted cation motion, making NMR a potentially useful technique for detecting different metal-binding sites. However, the conventional magic-angle spinning (MAS) ^{23}Na NMR technique still suffers from poor spectral resolution because of the incomplete averaging of second-order quadrupolar interactions.[7] Consequently, solid-state NMR of alkali metal nuclei has found little use in the study of biological systems. A recently developed solid-state NMR technique, the multiple-quantum magic-angle spinning (MQMAS) methodology, makes it possible to completely remove the undesirable second-order quadrupolar interactions for half-integer quadrupolar nuclei.[8] The tremendous improvement in spectral resolution brought about by the use of MQMAS has inspired new views concerning the potential of solid-state alkali metal NMR in many areas of chemistry and materials science.[9−20] Extension of the new high-resolution solid-state NMR techniques to the study of biological systems is also an emerging trend. For example, direct detection of the Na^+ ions bound to oligonucleotides containing G-quartet structures has been recently demonstrated.[21] To correctly interpret solid-state ^{23}Na NMR parameters and eventually relate them to the local structures at the binding site, it is desirable to examine a series of model systems for which the Na^+ binding sites are well defined. To this end, we have chosen to study sodium complexes with crown ethers, cryptands, and naturally occurring antibiotic ionophores by solid-state ^{23}Na NMR spectroscopy. Sodium complexes with ionophore ligands have been extensively studied for many years. More importantly, a large number of Na^+−ionophore complexes have been structurally characterized by X-ray crystallography.[22] Furthermore, because of the striking similarity among ion coordination environments in G-DNAs, K^+-specific binding proteins, and sodium ionophore complexes, the latter systems should serve as excellent models for establishing a correlation between solid-state ^{23}Na NMR parameters and ion-binding geometry. It should be pointed out that, although the correlation between solid-state ^{23}Na NMR parameters and molecular structure is well documented for inorganic sodium salts,[23,24] much less solid-state ^{23}Na NMR data is available for sodium complexes with "organic" ligands.

* Corresponding author. Phone, (613) 533-2644; Fax, (613) 533-6669; e-mail, gangwu@chem.queensu.ca.

10.1021/jp002096p CCC: $19.00
Published on Web 12/06/2000

SCHEME 1

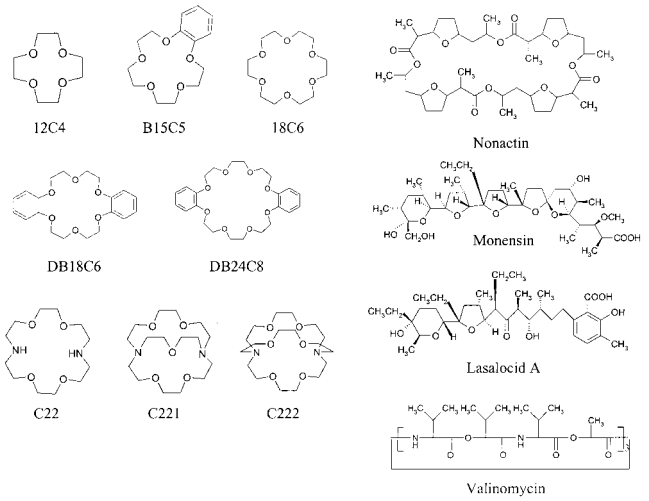

A considerable amount of literature can be found on solution ^{23}Na NMR studies of sodium complexes with synthetic and naturally occurring ionophores.[25−35] In contrast, the only solid-state ^{23}Na NMR study of Na−ionophore complexes was that by Saitô and co-workers.[36] Unfortunately, the low quality of the experimental spectra, obtained with NMR techniques available at the time, not only prevented these authors from obtaining any useful ^{23}Na quadrupole parameters, but also led to incorrect extraction of ^{23}Na chemical shifts. Clearly, a reexamination of alkali metal ionophore complexes, using modern solid-state NMR techniques, is in order. Also related to the present subject is the pioneering work of Dye and co-workers in solid-state ^{23}Na NMR studies of crystalline sodides.[37−39] In this contribution, we report a systematic solid-state ^{23}Na NMR study of a variety of sodium−ionophore complexes (Scheme 1).

2. Experimental Details

Sample Preparation. All crown-ether and cryptand ligands were purchased from Aldrich. Nonactin (from Streptomyces tsusimaensis), Valinomycin and Monensin sodium salt were obtained from Sigma. All sodium complexes were prepared according to the literature procedures.[40−46] Lasalocid A sodium salt was obtained from Aldrich and recrystallized from methanol before use.

MAS NMR. Solid-state ^{23}Na NMR spectra were obtained under the MAS condition on a Bruker Avance-500 NMR spectrometer operating at 132.295 MHz for ^{23}Na nuclei. A Bruker 4-mm MAS probe was used, with sample spinning speeds ranging between 6 and 12 kHz. Single-pulse excitation with a pulse length of 0.8 μs (approximately 30°) was used in obtaining ^{23}Na MAS spectra. Typical recycle delay times were 5−10 s. High-power proton decoupling was applied during data acquisition. All ^{23}Na chemical shifts were referenced to 0.1 M NaCl (aq) by setting the signal of a solid NaCl sample to δ = 7.21 ppm.[47] Spectral simulations were performed with the WSOLIDS program (Drs. Klaus Eichele and Rod Wasylishen, Dalhousie University).

MQMAS NMR. The pulse sequence containing two nutation pulses and a *z*-filter[48] was used in obtaining the ^{23}Na 3QMAS spectra: P1(ϕ1)-t1-P2(ϕ2)-τ-P3(ϕ3)-ACQ(t2, ϕ4) where ϕ1 = (0°); ϕ2 = (0, 0, 60, 60, 120, 120, 180, 180, 240, 240, 300, 300°); ϕ3 = (0, 180°); ϕ4 = (0, 180, 180, 0°), and τ = 20 μs. The optimized excitation (P1) and conversion (P2) pulse widths were 5.5 and 2.0 μs, respectively. The pulse width of the selective ^{23}Na 90° pulse (P3) was 19 μs. The sample spinning frequency was 10 kHz. A total of 240 transients were collected for each of the 56 t_1 increments with a recycle delay of 10 s. The two-dimensional (2D) data set was zero-filled to a size of 1024 × 128 before 2D shear Fourier transform (FT). The States hypercomplex data method[49] was used to obtain pure-phase 2D spectra.

3. Results and Discussion

In general, solid-state ^{23}Na NMR spectra of sodium−ionophore complexes were obtained using MAS and high-power proton decoupling. Under such circumstances, the observed central-transition ^{23}Na NMR spectra exhibit typical features arising from second-order quadrupole interaction. In most cases only a single Na^+ site is present in each of the complexes, making it possible to analyze the 1D MAS spectra in a straightforward way. From spectral analysis, isotropic ^{23}Na chemical shift (δ_{iso}), quadrupole coupling constant (QCC), and asymmetry parameter (η) can be obtained. In one case where multiple Na^+ sites were present, the MQMAS approach was then used to resolve the different sites. The solid-state ^{23}Na NMR parameters determined for the Na^+−ionophore complexes are summarized in Table 1, along with relevant structural data.

3.1. Chemical Shifts and Quadrupolar Coupling Constants. *Crown Ethers.* Solid-state ^{23}Na MAS spectra for Na(B15C5)I·H_2O, Na(18C6)SCN·H_2O and $Na(12C4)_2ClO_4$ are shown in Figure 1, along with the corresponding crystal structures. The definitions for different ionophore ligands are given in Scheme 1. The largest ^{23}Na chemical shift value observed for the present Na^+ crown-ether series is that in Na(B15C5)I·H_2O, δ = 13 ppm. The sodium ion in Na(B15C5)I·H_2O is coordinated by five oxygen atoms from the benzo-15-crown-5 molecule and one oxygen atom from the water molecule in a pentagonal pyramid fashion.[41] The Na−O_{ether} distances vary between 2.354 and 2.427 Å, and the sodium ion is 0.75 Å out of the crown-ether plane toward the apical water molecule, with a significantly shorter Na−O_W distance, 2.285 Å. It is interesting to note that the Na−O_W distance in Na(B15C5)I·H_2O is very similar to the sum of individual ionic radii for Na^+ (0.95 Å) and O (1.40 Å). This strong sodium−oxygen interaction may cause sufficient electron transfer from the oxygen atom to the 3p orbital of the sodium ion, increasing the paramagnetic shielding contribution to the ^{23}Na chemical shift. Consequently, the ^{23}Na NMR signal in Na(B15C5)I·H_2O is the most deshielded compared with other sodium complexes in this study (vide infra). The ^{23}Na QCC found for Na(B15C5)I·H_2O is 1.45 MHz with an asymmetry parameter of 0.50.

As seen in Figure 1B, the Na^+ ion in Na(18C6)SCN·H_2O is wrapped by the 18-crown-6 molecule, forming a distorted pentagonal bipyramid with a water molecule as an apical ligand.[42] In this complex, the Na−O_W distance is 2.321 Å, which is slightly longer than that in Na(B15C5)I·H_2O noted previously. The observed ^{23}Na chemical shift for Na(18C6)SCN·H_2O, δ = 1 ppm, is much smaller than that found for Na(B15C5)I·H_2O. Meanwhile, the ^{23}Na QCC for Na(18C6)SCN·H_2O is also smaller, at 0.95 MHz.

The ^{23}Na chemical shift for $Na(12C4)_2ClO_4$ is at −6 ppm, which represents a significantly shielded Na^+ environment compared with those in Na(B15C5)I·H_2O and Na(18C6)SCN·H_2O. In the crystal lattice, $Na(12C4)_2ClO_4$ exhibits a sandwich-like structure, with the sodium ion being coordinated by eight ether oxygen atoms from the two 12-crown-4 molecules;[40] see Figure 1C. The eight Na−O distances are quite similar, ranging from 2.474 to 2.534 Å. The rather symmetrical Na^+ coordination

TABLE 1: Summary of Solid-State ^{23}Na NMR Parameters, Structural Parameters, and Average Bond Valence Parameters (*A*) for the Sodium Complexes with Crown Ethers, Cryptands, and Natural Ionophores

complex	QCC (MHz)	η	δ_{iso} (ppm)	average r_{Na-O} (Å)	range r_{Na-O} (Å)	Na^+ coordination	A^a	structure ref
				Crown Ethers				
$Na(12C4)_2ClO_4$	1.10	0.00	−6	2.493	2.474−2.534	8O	0.1203	40
$Na(B15C5)I\cdot H_2O$	1.45	0.50	13	2.370	2.285−2.427	6O	0.1371	41
$Na(18C6)SCN\cdot H_2O$	0.95	1.00	1	2.516	2.321−2.623	7O	0.1140	42
$Na(DB18C6)Br\cdot 2H_2O$								
Site A	1.70	0.32	−13	2.60	2.27−2.82	8O	0.1077	43
Site B	3.35	0.15	−3	2.69	2.35−2.89	7O, 1Br		43
(Na-*o*-nitrophenolate)$_2$(DB24C8)	2.65	0.00	−4	2.439	2.296−2.615	6O	0.1137	44
				Cryptands				
Na(C22)SCN	1.60	1.00	−1			4O, 3N		50[b]
Na(C221)SCN			−3[c]	2.481	2.451−2.519	5O, 2N	0.1263	45
Na(C222)I	0.95	0.00	−9	2.574	2.566−2.582	6O, 2N	0.1159	46
Na(C222)SCN	0.94	0.50	−12			6O, 2N		
$Na(C222)Na^-$	1.268	0.00	−7[d]	2.57		6O, 2N	0.1185	51
				Natural Ionophores				
Na(lasalocid A)MeOH	1.40	1.00	−1			5O		53
Na(monensin)Br	1.65	0.75	−4	2.424	2.349−2.503	6O	0.1224	52
Na(valinomycin)SCN	3.15	0.60	2			6O		54[c]
Na(nonactin)SCN	0.58	1.00	−16	2.593	2.395−2.791	8O	0.1017	56

[a] A is defined in eq 2. [b] Based on corresponding potassium complexes. [c] From ref 55. [d] From ref 39.

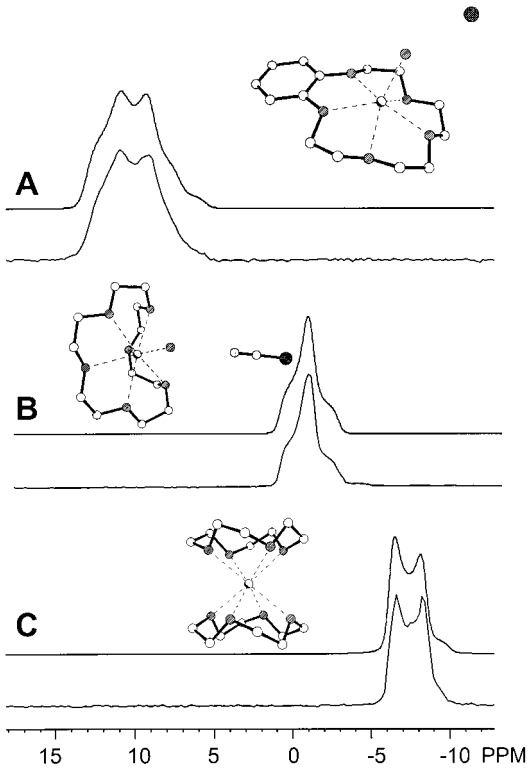

Figure 1. Experimental (lower trace) and calculated (upper trace) ^{23}Na MAS NMR spectra of (A) $Na(B15C5)I\cdot H_2O$, (B) $Na(18C6)SCN\cdot H_2O$, and (C) $Na(12C4)_2ClO_4$ at 11.75 T. The corresponding crystal structures are shown in the insets.

environment in $Na(12C4)_2ClO_4$ results in a small ^{23}Na QCC, 1.10 MHz. The electric field gradient (EFG) at the Na^+ site was also found to be axially symmetric ($\eta = 0$).

As illustrated in Figure 2, (Na-*o*-nitrophenolate)$_2$(DB24C8) contains two crystallographically equivalent sodium sites, both of which are located inside the large dibenzo-24-crown-8 ring.[44] Each of the sodium ions is coordinated with a total of six oxygen atoms. Two *o*-nitrophenolate ions bridge the two Na^+ ions from either side of the crown ring through nitro and phenolate groups. The $Na-O_{ether}$ distances range from 2.468 to 2.615 Å, whereas the nitro oxygen and the negatively charged phenolate oxygen

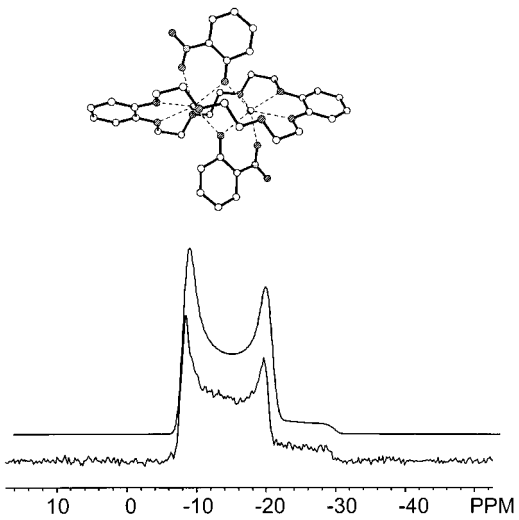

Figure 2. Experimental (lower trace) and calculated (upper trace) ^{23}Na MAS NMR spectra of (Na-*o*-nitrophenolate)$_2$(DB24C8) at 11.75 T. The corresponding crystal structure is shown in the inset.

are at 2.399 and 2.296 Å from the Na^+ ion, respectively. The ^{23}Na chemical shift is −4 ppm. The ion−ion interaction between the two Na^+ ions separated by 3.383 Å appears to have negligible effects on the ^{23}Na chemical shift. A relatively large ^{23}Na QCC, 2.65 MHz, is observed for (Na-*o*-nitrophenolate)$_2$-(DB24C8), which apparently results from a very distorted Na^+ coordination environment. The ^{23}Na NMR spectrum of this complex, shown in Figure 2, clearly indicates that $\eta = 0$. However, the reason that the EFG at the Na^+ site in this complex has an axial symmetry is not obvious.

The ^{23}Na MAS spectrum of $Na(DB18C6)Br\cdot 2H_2O$ (shown in Figure 3D) exhibits some complex features that suggesting the presence of multiple Na^+ sites. The crystal structure of $Na(DB18C6)Br\cdot 2H_2O$ indicates that two Na^+ sites with different coordination environments exist.[43] Each of the two Na^+ sites can be described as being at the center of a hexagonal bipyramid. However, one sodium site (Na_A) is coordinated by two water molecules as axial ligands, whereas the other sodium site (Na_B) has one water molecule and one bromide ion as axial ligands. The two independent complex molecules are linked by a

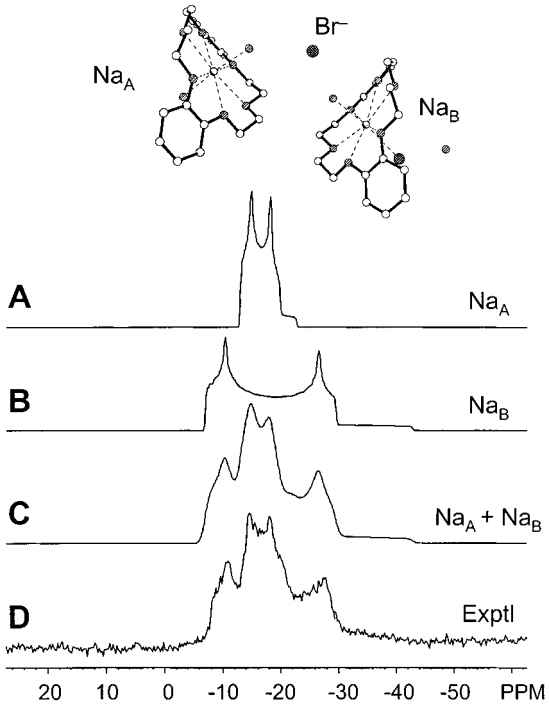

Figure 3. Calculated (A, B, C) and experimental (D) ^{23}Na MAS spectra of Na(DB18C6)Br·2H_2O at 11.75 T.

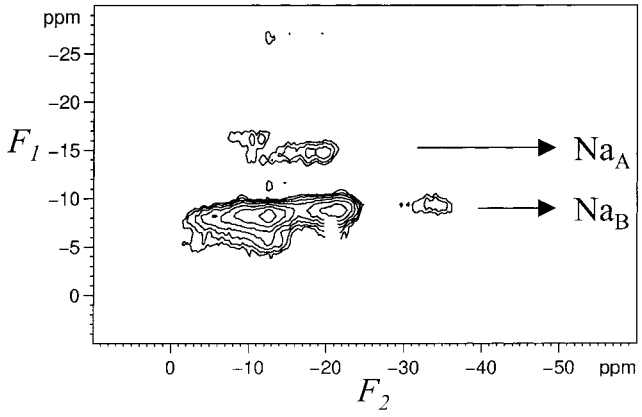

Figure 4. Two-dimensional ^{23}Na MQMAS NMR spectrum of Na(DB18C6)Br·2H_2O at 11.75 T. F_2 corresponds to the normal MAS dimension, whereas F_1 is the isotropic dimension.

bromide ion in the following fashion:

$$H_2O{-}Na_A{-}H_2O \cdots Br^{-}\cdots H_2O{-}Na_B{-}Br^{-}$$

where the O_W−bromide distances are 3.29 and 3.27 Å and the $O_W{-}Br^{-}{-}O_W$ angle is 113°.[43] Because of the presence of two Na^+ sites in Na(DB18C6)Br·2H_2O, analysis of the ^{23}Na MAS spectrum was not straightforward. In fact, we found two sets of parameters that can reproduce the experimental ^{23}Na MAS spectrum equally well. To resolve this ambiguity, we obtained a two-dimensional (2D) MQMAS spectrum for Na(DB18C6)-Br·2H_2O. As shown in Figure 4, the 2D MQMAS spectrum clearly indicates the presence of two different sodium sites. From the two F_1 slice spectra, it is a straightforward task to extract ^{23}Na NMR parameters for the two sites: Na_A, $\delta = -13$ ppm, QCC = 1.70 MHz, and $\eta = 0.32$; Na_B, $\delta = -3$ ppm, QCC = 3.35 MHz, and $\eta = 0.15$. We tentatively assign Na_A to be the sodium site bound to two axial water molecules, because this site is clearly more "symmetrical" than the other sodium site for which one water and one negatively charged bromide ion

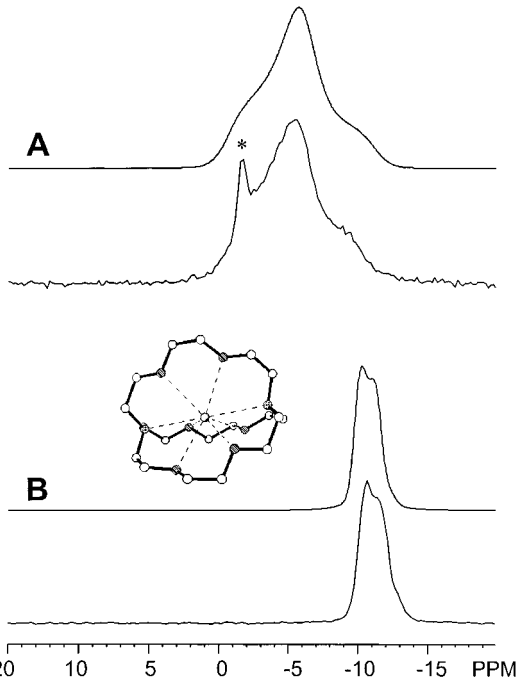

Figure 5. Experimental (lower trace) and calculated (upper trace) ^{23}Na MAS NMR spectra of (A) Na(C22)SCN and (B) Na(C222)I at 11.75 T. The crystal structure of Na(C222)I is shown in the inset. In (A), the asterisk indicates the presence of a small amount of NaSCN.

serve as axial ligands. It is also noted that, because of the strong ion−ion interaction between Na^+ and Br^- (2.82 Å), the Na_B ion is out of the 18-crown-6 plane by 0.27 Å toward the bromide ion. In contrast, Na_A is only 0.07 Å out of the 18-crown-6 plane. Another piece of evidence supporting our assignment is that, although the sodium−oxygen distances around Na_B vary between 2.54 and 2.89 Å, the sodium−oxygen distances for Na_A are within a much smaller range, 2.63−2.82 Å. Therefore, Na_A is expected to exhibit a smaller QCC. It is also interesting to note from the 2D ^{23}Na MQMAS spectrum that the peak arising from Na_B exhibits a larger line width in the isotropic F_1 dimension. This additional broadening presumably is due to the residual dipolar coupling to a neighboring quadrupolar nucleus, $^{79/81}$Br ($I = 3/2$).[57−59]

Cryptands. Figure 5 shows ^{23}Na MAS spectra for two typical sodium−cryptand complexes. The ^{23}Na chemical shift for Na(C22)SCN is found to be −1 ppm, and the ^{23}Na QCC is 1.60 MHz. No structural data are available for Na(C22)SCN; however, this Na^+ complex may have a structure similar to that of K(C22)SCN. It is known that K(C22)SCN has a hexagonal pyramid structure, wherein the K^+ ion is coordinated with four oxygen and two nitrogen atoms from the cryptand molecule.[50] In addition, the SCN^- ion serves as an apical ligand. Because the ionic radius of Na^+ (0.95 Å) is much smaller than that of K^+ (1.33 Å), the Na^+ ion may experience a more distorted hexagonal pyramid environment in a cavity of 5.84 Å than does K^+ in K(C22)SCN. This may explain the observation of a relatively large ^{23}Na QCC for Na(C22)SCN.

As seen in Figure 5B, the ^{23}Na NMR signal of Na(C222)I, $\delta_{iso} = -9$ ppm, is more shielded than that of Na(C22)SCN. The ^{23}Na QCC for Na(C222)I, 0.95 MHz, is also smaller than that in Na(C22)SCN. Na(C222)I crystallizes in the hexagonal system with space group $P31c$.[46] The Na^+ ion is trapped inside the C222 cage with a Na−O distance range of 2.566−2.582 Å. The two Na^+−N distances are 2.722 and 2.782 Å. The crystallographic symmetry at the Na^+ ion is C_3. Therefore, the observation that $\eta = 0$ for Na(C222)I is in agreement with the

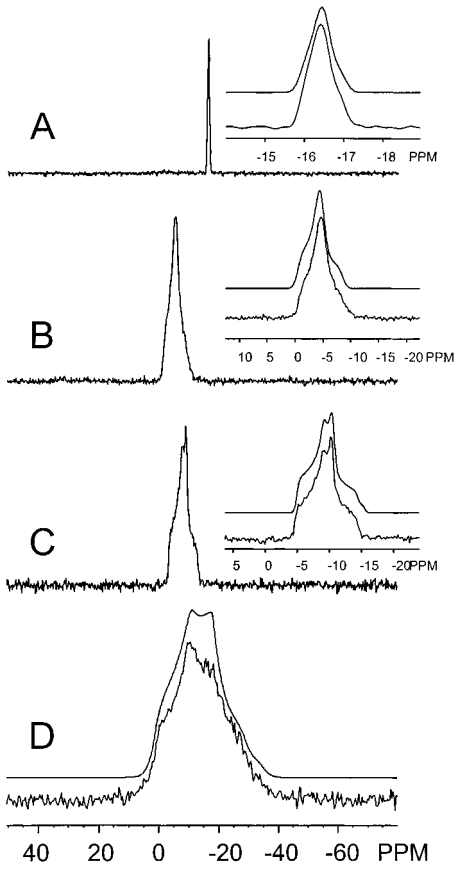

Figure 6. Experimental (lower trace) and calculated (upper trace) ^{23}Na MAS NMR spectra of (A) Na(nonactin)SCN, (B) Na(lasalocid A)·MeOH, (C) Na(monesin)Br, and (D) Na(valinomycin)SCN at 11.75 T.

crystal data. Similar to Na(C222)I, the ^{23}Na NMR spectrum of Na(C222)SCN (spectrum not shown) exhibits $\delta_{iso} = -12$ ppm. No crystal parameters are available in the literature for Na(C222)SCN. However, on the basis of the similarity between the ^{23}Na NMR parameters for Na(C222)SCN and Na(C222)I, we can conclude that the two compounds must have similar structures, except that the former complex does not possess a 3-fold site symmetry as suggested by its nonaxially symmetric EFG ($\eta = 0.5$). Some time ago, Kim and Dye[39] reported a single-crystal ^{23}Na NMR study of Na(C222)Na$^-$. They found $\delta = -7$ ppm and QCC = 1.268 MHz with $\eta = 0$. The crystal structure of Na(C222)Na$^-$ indicates that the sodium ion is well-caged inside the cryptand cavity and well-separated from the counterion.[51] It is interesting to note that both ^{23}Na QCCs and chemical shifts for Na(C222)I and Na(C222)SCN are comparable to the values found in Na(C222)Na$^-$. This similarity suggests that the anion has little effect on the chemical environment at the Na$^+$ site in Na(C222)X complexes.

Naturally Occurring Antibiotic Ionophores. The above discussions have focused on sodium complexes with relatively simple crown-ether and cryptand ligands. Now we examine several sodium complexes with more complex ligands. In particular, we will study sodium complexes with four naturally occurring antibiotic ionophores: lasalocid A, monensin, valinomycin, and nonactin. Solid-state ^{23}Na MAS spectra of these complexes are shown in Figure 6. The ^{23}Na MAS spectrum of the Na$^+$−nonactin complex (Figure 6A) exhibits a sharp peak from which the following ^{23}Na quadrupole parameters were determined: QCC = 0.58 MHz and $\eta = 1.0$. The ^{23}Na chemical shift found for the Na$^+$−nonactin complex, −16 ppm, is the most shielded value observed for the Na$^+$−ionophore complexes. Saitô and Tabeta[55] also reported a similar ^{23}Na chemical shift value for Na$^+$−nonactin in chloroform solution, −12 ppm. The observation of a remarkably shielded Na$^+$ ion is certainly related to the Na$^+$ coordination environment in the Na$^+$−nonactin complex. The Na$^+$ ion is at the center of an approximate cube whose eight corners are four ether− and four carbonyl−oxygen atoms.[56] The average Na−O distance, 2.593 Å, is relatively long compared with the corresponding values found in other Na$^+$ complexes. It is interesting to note that the Na$^+$ ion in Na(12C4)$_2$ClO$_4$ is at the center of a similar cube. However, the ^{23}Na chemical shift observed for Na(12C4)$_2$ClO$_4$, −6 ppm, is quite different from that for Na(nonactin)SCN, −16 ppm. This discrepancy must arise from the different nature of the oxy ligands and the different ion-binding geometry present in the two complexes (vide infra). Na(lasalocid A)·MeOH crystallizes in the orthorhombic system with space group $P2_12_12_1$.[53] The Na$^+$ ion is coordinated by six oxygen atoms: two ethers, one carbonyl and three hydroxyl groups. The methanol molecule plays the role of capping the Na$^+$ ion. The ^{23}Na chemical shift and QCC for Na(lasalocid A)·MeOH are −1 ppm and 1.40 MHz, respectively. As seen in Figure 6B, the ^{23}Na MAS NMR spectrum of Na(lasalocid A)·MeOH also exhibits $\eta = 1.0$. For the Na−monensin complex, the Na$^+$ ion is coordinated by four ether oxygen atoms and two hydroxyl groups forming a distorted octahedron.[52] There is no distinct difference between the Na−O$_{ether}$ and Na−O$_{hydroxyl}$ distances. From the spectrum shown in Figure 6C, the ^{23}Na chemical shift and QCC were determined to be −4 ppm and 1.65 MHz, respectively. These parameters are quite similar to those found in Na(lasalocid A)·MeOH. As seen in Figure 6D, the Na-(valinomycin)SCN complex exhibits the largest ^{23}Na QCC in the series, 3.15 MHz, whereas the ^{23}Na chemical shift is +2 ppm. No crystal parameters are available in the literature for this sodium complex. However, the crystal structure of K(valinomycin)SCN is known[54] where the K$^+$ ion is coordinated by six carbonyl oxygen atoms from the ester groups in a nearly regular octahedral structure. However, the large ^{23}Na QCC observed in Na(valinomycin)SCN suggests considerable distortion at the Na$^+$ site, which may arise from the smaller ionic radius of Na$^+$ or/and from neighboring hydrogen bonding between the amide N−H and the ester C═O groups. The large ^{23}Na QCC in the Na$^+$−valinomycin complex is consistent with the results from previous solution ^{23}Na NMR studies.[25,55] Clearly because of the large chemical and structural variations among the four naturally occurring antibiotic ionophores, a large ^{23}Na QCC range was observed for these complexes, 0.58−3.15 MHz.

Chemical-Shift Anisotropy. Because of the small chemical-shift range of ^{23}Na nuclei, only two reports have appeared in the literature concerning the determination of ^{23}Na chemical-shift anisotropy (CSA) in inorganic Na$^+$ salts.[60] It is also of interest to examine ^{23}Na CSA in Na$^+$−ionophore complexes. Because the ^{23}Na EFG tensor is axially symmetric in Na(12C4)$_2$ClO$_4$ ($\eta = 0$), this compound is an ideal system for demonstrating the determination of ^{23}Na CSA. The stationary ^{23}Na NMR spectrum of Na(12C4)$_2$ClO$_4$ is shown in Figure 7. Because the ^{23}Na quadrupole parameters have been determined from analysis of the ^{23}Na MAS spectra, the only adjustable parameters in the analysis of the stationary ^{23}Na NMR spectrum are the chemical-shift tensor components. Analysis yields the following parameters: $\delta_{11} = \delta_{22} = -1$ ppm and $\delta_{33} = -15$ ppm. As seen from Figure 7, the span of this ^{23}Na chemical-shift tensor contributes approximately 1.8 kHz (at 11.75 T) to the total line width (3.2 kHz) of the stationary NMR spectrum of Na(12C4)$_2$ClO$_4$. Our observation also follows the same trend

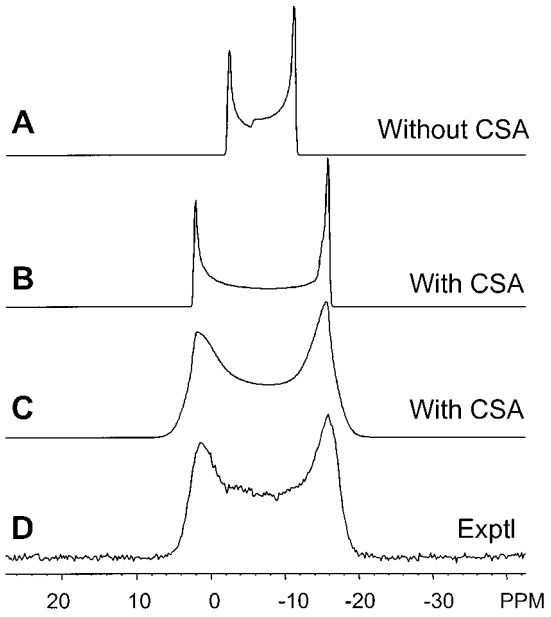

Figure 7. Calculated (A, B, C) and experimental (D) ^{23}Na NMR spectra of a stationary powder sample of $Na(12C4)_2ClO_4$ at 11.75 T.

as in inorganic salts,[60] that the unique ^{23}Na chemical-shift tensor component corresponds to the direction with the largest shielding. Because the absolute ^{23}Na shielding scale has been established,[61] it might be possible to use the reported tensor components for $Na(12C4)_2ClO_4$ as a test for the quality of modern ab initio ^{23}Na chemical-shielding calculations.

3.2. Interpretation of the ^{23}Na Chemical Shifts. A considerably large amount of literature exists concerning NMR chemical shifts of alkali metal nuclei both in the liquid phase[28−35] and in the solid state.[22,23,35] In addition, theoretical work on alkali metal chemical shifts in metal halides can also be traced back to the early years of NMR.[62−65] However, it is noteworthy that previous solid-state ^{23}Na NMR studies have focused only on inorganic systems. In this section, we will discuss the interpretation of the observed ^{23}Na chemical shifts for Na^+−ionophore complexes.

Numerous ^{23}Na NMR studies have established a general trend in ^{23}Na chemical shifts: the ^{23}Na chemical shift decreases with increasing correlation number (CN) and increasing Na−O distance.[22,23,32−34] In a recent study, Tossell[66] performed gauge-invariant atomic orbital (GIAO) ^{23}Na shielding calculations for $[Na(H_2O)_n]^+$ clusters where n = 0, 2, 4, 5, 6, and 8. The theoretical result indicated that the ^{23}Na chemical shift is decreased by 5 ppm/water as n increases from 4 to 8. It would be of great interest to examine the possibility of carrying out ab initio ^{23}Na shielding calculations for Na−ionophore complexes. Unfortunately, our current computation resource does not permit us to perform ab initio ^{23}Na shielding calculations for the large molecular systems studied here. Therefore, at this stage we attempted only to find an empirical structural parameter that may be related to ^{23}Na chemical shifts.

To improve the general correlation between the ^{23}Na chemical shift and structural data, it is necessary to take into account the different electronic environment for different ligands. For example, a nitrogen ligand will certainly have a different effect on the ^{23}Na chemical shift compared to an oxygen ligand. Recently, Koller et al.[24] found a correlation between the ^{23}Na chemical shift and an empirical bond valence parameter for inorganic sodium salts. However, using the same parameter, we found no clear correlation with the data shown in Table 1. For this reason we use a slightly different approach. We assume

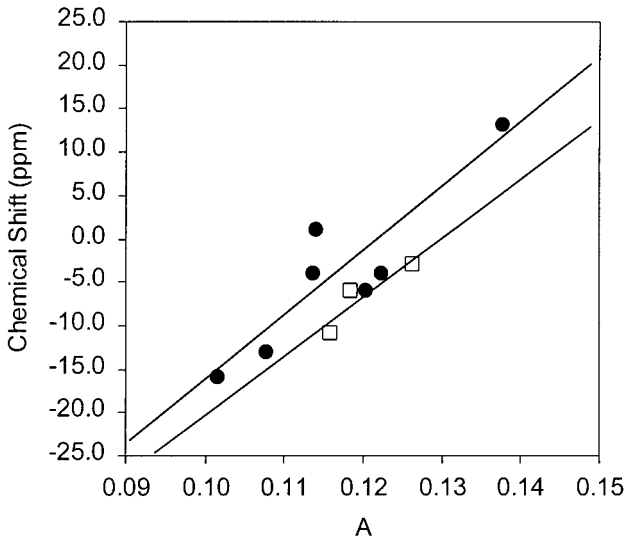

Figure 8. Correlation between the experimental ^{23}Na chemical shift and A for sodium−oxygen (closed circles) and sodium−oxygen/nitrogen (open squares) complexes.

that the specific contribution from a donor atom (either oxygen or nitrogen in the present case) to the ^{23}Na chemical shift is related to the atomic valence (W_i) of the donor atom in the absence of the interaction with the Na^+ ion. For a particular functional group, W_i can be calculated from a sum of all bond valences (s_{ij}):

$$W_i = \Sigma s_{ij} = \Sigma \exp[(r_o - r_{ij})/0.37] \quad (1)$$

where r_o is an empirical parameter and can be found in ref 67, and r_{ij} is the bond distance between atoms j and i. The only difference in W_i calculations between our approach and that of Koller et al.[24] is that we exclude the Na-donor bond. For sodium−ionophore complexes, the Na^+ ions are generally coordinated by oxygen atoms from ether, carbonyl, nitro, and hydroxyl groups as well as by nitrogen atoms in the case of cryptands. W_i allows one to differentiate contributions from different functional groups. The order of the average oxygen atomic valence, W_i, for the functional groups encountered in this study is as follows: ether (1.849) > hydroxyl (1.723) > carbonyl (1.717) > water (1.620) > nitro (1.480) > carbonate (1.364). As mentioned before, because the ^{23}Na chemical shift also depends on Na-donor distances within the first-coordination sphere and CN, we define an average bond valence parameter, A, as

$$A = \frac{\sum W_i r_i^{-3}}{\mathrm{CN}} \quad (2)$$

where r_i is the distance between the Na^+ ion and the donor atom with W_i. It should be noted that the inverse dependence of the A parameter on CN was not considered by Koller et al.[24] The recent theoretical study of Tossell[66] on $[Na(H_2O)_n]^+$ clusters clearly suggested that both Na−ligand distance and CN are important.

Figure 8 shows the correlation between the experimental ^{23}Na chemical shifts and the average bond valence parameters, A, for the Na complexes studied here. Clearly the ^{23}Na chemical shift increases with the value of A. For example, the combination of short Na−O distances, 2.285−2.427 Å, around the Na^+ ion in $Na(B15C5)I\cdot H_2O$ and a small CN, 5, gives rise to a large A value, and, consequently, the complex exhibits the most positive chemical shift, 13 ppm. On the other hand, although the two

TABLE 2: Comparison between Solution[a] and Solid-State[b] ^{23}Na NMR Parameters for Sodium Ionophore Complexes

	$CDCl_3$ solution		MeOH solution		solid state	
complex	δ/ppm	P_Q/MHz[c]	δ/ppm	P_Q/MHz	δ/ppm	P_Q/MHz
Na(18C6)SCN·H_2O	−10.9	1.9	−10.3	2.4	1	1.10
Na(C22)SCN	−5.0	3.3	−3.0	1.2	−1	1.84
Na(C222)I	−12.2	1.4	−10.3	1	−11	0.98
Na(lasalocid A)MeOH	−6.2	2.2	−4.0	0.94	−1	1.61
Na(monensin)Br	−12.4	2	−0.7	1.7	−4	1.80
Na(valinomycin)SCN	−7.7	4.7	−2.6	0.86	2	3.33
Na(nonactin)SCN	−12.1	0.82	−6.3	0.75	−16	0.67

[a] From ref 55. [b] This work. [c] P_Q is defined in eq 4.

Na−O_W distances for the Na_A site in Na(DB18C6)Br·$2H_2O$ are quite short, 2.27 and 2.31 Å, the relatively long Na−O_{ether} distances, 2.64−2.82 Å, coupled with a large CN, lead to a small *A* value, which explains the observation of a very negative chemical shift, −13 ppm. As mentioned earlier, the Na^+ ions in $Na(12C4)_2ClO_4$ and Na(nonactin)SCN both are coordinated by eight oxygen atoms. However, the ^{23}Na chemical shift of $Na(12C4)_2ClO_4$ is −6 ppm, which is considerably deshielded compared with that of Na(nonactin)SCN, −16 ppm. This discrepancy can be understood on the basis of the average bond valence parameter, *A*. First, four of the eight oxygen ligands in the Na−nonactin complex are carbonyls, which have smaller W_i than ether groups. Second, the Na−O_{ether} distances in the Na−nonactin complex, 2.744−2.791 Å, are much larger than the values of 2.474−2.534 Å found in the Na−12C2 complex. As seen from eq 2, the combination of these two factors results in a much smaller *A* parameter for Na(nonactin)SCN than for $Na(12C4)_2ClO_4$. As is also seen from Figure 8, the Na−cryptand complexes exhibit the same trend but with a slightly different offset. Nevertheless, our observation is also consistent with the results from a previous solution ^{23}Na NMR study of cryptands.[26] Similar chemical-shift dependencies have also been observed for ^{39}K, ^{87}Rb, and ^{133}Cs.[68,69] Early solution NMR studies[70,71] also suggested a correlation between the Gutmann donor number[72] of the solvent and ^{23}Na chemical shifts.

The general trend observed in Figure 8 can also be rationalized in a qualitative fashion with chemical-shielding theory. According to Ramsey's formula,[73] the origin of ^{23}Na chemical shielding can be written as a sum of diamagnetic and paramagnetic contributions. The diamagnetic shielding term arises from the induced motion of a spherically symmetric electron cloud at the nucleus of interest, whereas the paramagnetic shielding is caused by mixing of the electronic ground state with excited states by a strong external magnetic field. Usually the paramagnetic shielding term is responsible for variations of chemical shifts observed in different chemical compounds. To a very crude approximation, the paramagnetic shielding term, σ^P, can be written as[74−76]

$$\sigma^P \propto -(1/\Delta E)\langle 1/r^3\rangle \rho_e \qquad (3)$$

where ΔE is the average energy gap between the ground state and excited states of the molecule, $\langle 1/r^3\rangle$ is the average distance between electrons and the nucleus of interest, and ρ_e is the relative electron densities of the various p orbitals involved in bonding. For the ^{23}Na chemical shift, it is most likely that the paramagnetic shielding from interactions of electron donors and the empty p orbitals of the Na^+ ion is a dominant contributor. Therefore, it is reasonable that the average bond valence parameter, *A* (defined in eq 2), contains W_i and $1/r^3$. It is also noted that the explicit dependence on CN is not obvious from the chemical-shielding theory. However, it is a common observation that the average Na−donor distance increases with CN. Perhaps the inverse dependence of *A* on CN is caused by an indirect effect of CN on the Na−donor separation. The ^{23}Na chemical shift of −3 ppm for Na_B in Na(DB18C6)Br·$2H_2O$ deviates significantly from the plot shown in Figure 8. This difference apparently results from the uniquely strong ionic interaction between the Na^+ cation and the Br^- anion. The separation between the Na^+ and Br^- ions is 2.82 Å, which is considerably shorter than the sum of the ionic radii of the two ions, 2.93 Å.

3.3. Comparison between Solution and Solid-State ^{23}Na NMR Parameters. As mentioned earlier, one of the major problems of solution ^{23}Na NMR arises from the complexity of dynamic processes occurring in solution. Traditionally, ^{23}Na QCCs can be deduced from solution NMR relaxation studies. The drawback of such an approach is twofold. First, one needs to determine the rotational correlation time of the molecular complex. Second, any exchange process often complicates the relaxation data analysis. Now because we have obtained a set of accurate ^{23}Na NMR parameters for Na^+ sites with well-defined coordination environments, it will be interesting to compare our solid-state ^{23}Na NMR data with those obtained from previous solution NMR studies. A similar attempt was made previously by Saitô and Tabeta.[55] Unfortunately, these authors used incorrect solid-state ^{23}Na NMR data.

Solution and solid-state ^{23}Na NMR parameters for several Na−ionophore complexes are summarized in Table 2. In the discussion that follows, we use a combined quadrupole parameter, P_Q, defined by eq 4. We use this parameter because solution NMR relaxation studies are incapable of providing QCC and η separately.

$$P_Q = \mathrm{QCC} \times \sqrt{1 + \frac{\eta^2}{3}} \qquad (4)$$

One of the interesting observations illustrated in Figure 9 is that, although the quadrupole parameters obtained from $CDCl_3$ solutions show a nice correlation with the solid-state data, no correlation exists between MeOH solution data and solid-state data. This observation is in agreement with the previous knowledge that the Na^+ cation-exchange process is much slower in $CDCl_3$ than in MeOH.[55] The observed correlation strongly supports the idea that, on the NMR time scale, the Na^+ ion-coordination environment for Na−ionophore complexes is very similar in a hydrophobic solvent ($CDCl_3$) to that in the crystal lattice. As seen from Figure 9, the plot has a slope of 1.41. The higher ^{23}Na QCC values found in $CDCl_3$ may be attributed to uncertainties arising either from measurement or from a molecular dynamic effect. Nevertheless, the drastically different ^{23}Na QCC values in $CDCl_3$ and MeOH clearly illustrate the different solution behaviors of Na−ionophore complexes in hydrophobic and hydrophilic solvents. Interestingly, Na(C222)I, Na(monensin)Br, and Na(nonactin)SCN exhibit very similar ^{23}Na QCCs in both solvents and in the solid state.

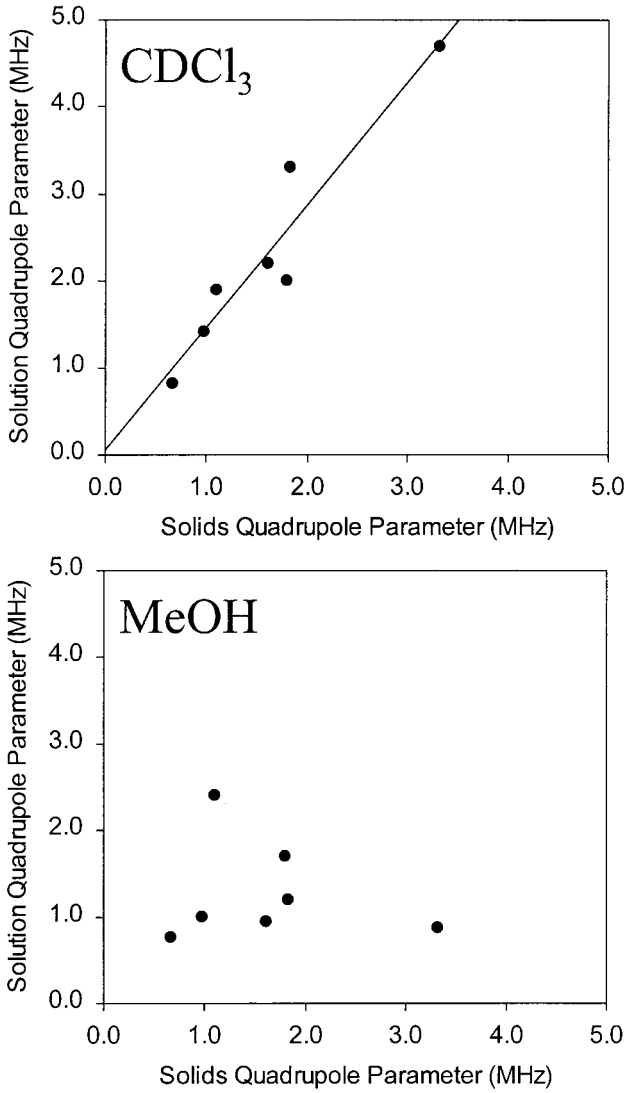

Figure 9. Solution versus solid-state ^{23}Na quadrupole parameters.

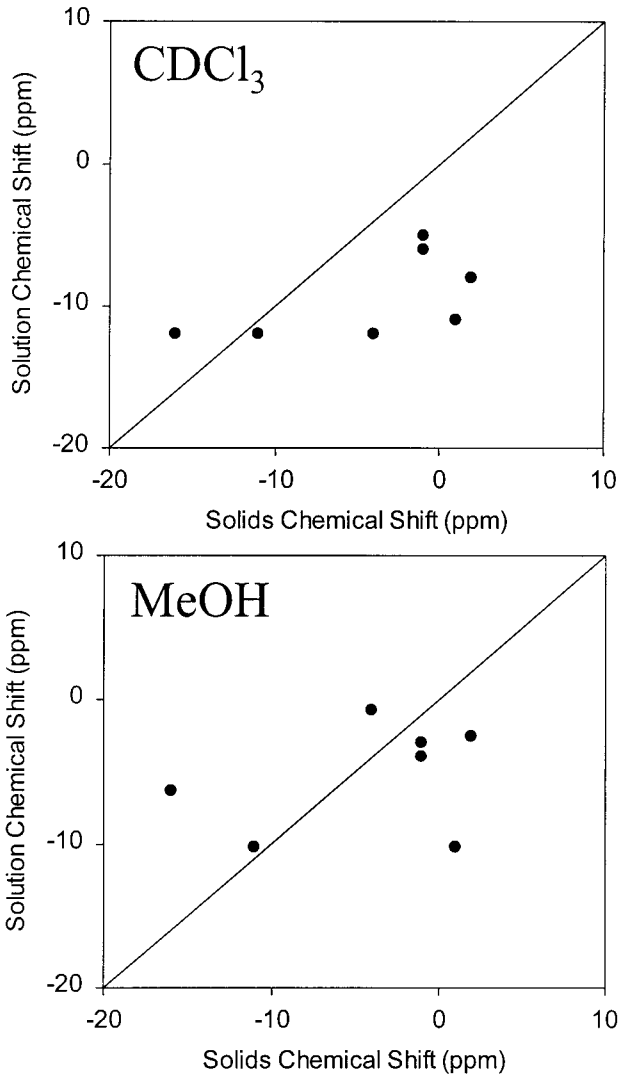

Figure 10. Solution versus solid-state ^{23}Na chemical shifts. The diagonal lines are shown for easy comparison.

Inspection of the ^{23}Na chemical shifts shown in Table 2 also reveals some interesting trends. As shown in Figure 10, the ^{23}Na chemical shifts obtained from $CDCl_3$ solution are consistently smaller than the solid-state values, except for the Na−nonactin complex. This observation is opposite to the conclusion of Saitô and Tabeta.[55] The discrepancy arises from their incorrect interpretation of ^{23}Na chemical shifts from solid-state NMR spectra. However, using the same explanation as proposed by Saitô and Tabeta,[55] we may speculate that the conformation of Na−ionophore complexes expands slightly in $CDCl_3$ solution compared to that in the crystal lattice. Once again, the Na−C222 complex exhibits essentially identical chemical shifts in solution and in the solid state, indicating that there is very little conformation change in solution for this sodium complex. This is certainly understandable from its cage like structure. In contrast, the Na-18C6 complex exhibits the largest chemical-shift discrepancy between solution data and solid-state values, suggesting that the flat structure of the 18C6 molecule renders cation exchange more likely to occur. In MeOH solution, no clear correlation exists between solution chemical shifts and solid-state data. The rapid exchange processes in MeOH made it difficult to interpret the observed ^{23}Na chemical shifts.

Finally, we address the issue of sensitivity concerning solid-state ^{23}Na NMR experiments, especially the new MQMAS approach, in the study of large biomolecular systems. The largest molecular system presented in this contribution is the sodium complex of valinomycin, a cyclic dodecadepsipeptide with a molecular weight of approximately 1.2 kDa. Because this complex also exhibits the largest ^{23}Na QCC, it is reasonable to use it as a benchmark for predicting the feasibility of solid-state ^{23}Na NMR for even larger biomolecular systems. For a sample of approximately 10 mg Na(valinomycin)SCN, we found that it takes only a few minutes to record a ^{23}Na MAS NMR spectrum (at 11.75 T) with a reasonable signal-to-noise (S/N) ratio. With a relatively high B_1 field (100 kHz), the triple-quantum (3Q) excitation and 3Q-to-1Q conversion can be achieved with reasonably high efficiencies. Therefore, it can be concluded that, with modern high-field spectrometers ($\geq$11.75 T), two-dimensional MQMAS-based ^{23}Na NMR techniques will be applicable to biomolecular systems with 100 kDa.

4. Conclusions

We have reported a systematic solid-state ^{23}Na NMR study of sodium complexes with synthetic and naturally occurring ionophores. Attempts have been made to relate the ^{23}Na chemical shifts to structural data. In contrast to the traditional solution ^{23}Na NMR techniques, the advantage of solid-state ^{23}Na NMR lies on its capability of providing direct and precise information about the Na^+ binding sites. We have also demonstrated the utility of 2D MQMAS ^{23}Na NMR in studying

Na−ionophore complexes. The experimental data presented in this contribution provide useful benchmark NMR parameters for different Na^+ binding sites. Our results will be useful in interpreting solid-state ^{23}Na NMR parameters (chemical shift and QCC) from other related systems. Although it is common knowledge that the relative sensitivity of ^{23}Na NMR is high, the information from traditional solution ^{23}Na NMR studies of biological systems is always very limited, largely because of the small ^{23}Na chemical-shift range and the dynamic nature of solution samples. In light of the present results, we anticipate that solid-state ^{23}Na NMR at high fields will become increasingly important in the study of Na^+ binding to biological macromolecules. The benefit of very high magnetic fields is to increase both the ^{23}Na chemical shift dispersion and the overall sensitivity of multidimensional NMR experiments.

Acknowledgment. We are grateful to the Natural Sciences and Engineering Research Council (NSERC) of Canada for research and equipment grants. A.W. thanks Queen's University for an R. S. McLaughlin Fellowship. G.W. thanks Queen's University for a Chancellor's Research Award and the Government of Ontario for a Premier's Research Excellence Award.

References and Notes

(1) Williamson, J. *Annu. Rev. Biophys. Biomol. Struct.* **1994**, *23*, 703 and references therein.
(2) Kang, C.; Zhang, X.; Ratliff, R.; Moyzis, R.; Rich, A. *Nature* **1992**, *356*, 126.
(3) Laughlan, G.; Murchie, A. I. H.; Norman, D. G.; Moore, M. H.; Moody, P. C. E.; Lilley, D. M. J.; Luisi, B. *Science* **1994**, *265*, 520.
(4) Philips, K.; Dauter, Z.; Murchie, A. I. H.; Lilley, D. M. J.; Luisi, B. *J. Mol. Biol*. **1997**, *273*, 171.
(5) Chaput, J. C.; Switzer, C. *Proc. Natl. Acad. Sci. U.S.A.* **1999**, *96*, 10614.
(6) (a) Toney, M. D.; Hohenester, E.; Cowan, S. W.; Jansonius, J. N. *Science* **1993**, *261*, 756. (b) Doyle, D. A.; Cabral, J. M.; Pfuetzner, R. A.; Kuo, A.; Gulbis, J. M.; Cohen, S. L.; Chait, B. T.; MacKinnon, R. *Science* **1998**, *280*, 69.
(7) (a) Freude, D.; Haase, J. In *NMR Basic Principles and Progress*; Diehl, P., Fluck, E., Günther, H., Kosfeld, R., Seelig, J., Eds.; Springer-Verlag: Berlin, 1993; Vol. 29, pp 1−90. (b) Chmelka, B. F.; Zwanziger, J. W. In *NMR Basic Principles and Progress*; Diehl, P., Fluck, E., Günther, H., Kosfeld, R., Seelig, J., Eds.; Springer-Verlag: Berlin, 1994; Vol. 33, pp 79−124.
(8) Frydman, L.; Harwood, J. S. *J. Am. Chem. Soc*. **1995**, *117*, 5367.
(9) Medek, A.; Harwood, J. S.; Frydman, L. *J. Am. Chem. Soc*. **1995**, *117*, 12779.
(10) Fernandez, C.; Amoureux, J.-P. *Chem. Phys. Lett*. **1996**, *242*, 449.
(11) Massiot, D.; Touzo, B.; Trumeau, D.; Coutures, J. P.; Virlet, J.; Florian, P.; Grandinetti, P. J. *Solid State Nucl. Magn. Reson*. **1996**, *6*, 73.
(12) Wu, G.; Rovnyak, D.; Sun, B. Q.; Griffin, R. G. *Chem. Phys. Lett*. **1996**, *249*, 210.
(13) Wu, G.; Rovnyak, D.; Griffin, R. G. *J. Am. Chem. Soc*. **1996**, *118*, 9326.
(14) Brown, S. P.; Heyes, S. J.; Wimperis, S. *J. Magn. Reson. Ser., A* **1996**, *119*, 280.
(15) Massiot, D. *J. Magn. Reson., Ser. A* **1996**, *122*, 240.
(16) Duer, M. J.; Stourton, C. *J. Magn. Reson*. **1997**, *124*, 189.
(17) Brown, S. P.; Wimperis, S. *J. Magn. Reson*. **1997**, *128*, 42.
(18) Amoureux, J.-P.; Fernandez, C. *Solid State Nucl. Magn. Reson*. **1998**, *10*, 211.
(19) Wu, G. *Biochem. Cell Biol.* **1998**, *76*, 429.
(20) Ding, S.; McDowell, C. A. *Chem. Phys. Lett*. **2000**, *320*, 316.
(21) Rovnyak, D.; Baldus, M.; Wu, G.; Hud, N. V.; Feigon, J.; Griffin, R. G. *J. Am. Chem. Soc*. **2000**, *122*, 11423.
(22) Dobler, M. *Ionophores and Their Structures*; Wiley: New York, 1981.
(23) Xue, X.; Stebbins, J. F. *Phys. Chem. Miner*. **1993**, *20*, 297.
(24) Koller, H.; Engelhardt, G.; Kentgens, A. P. M.; Sauer, J. *J. Phys. Chem*. **1994**, *98*, 1544.
(25) Erlich, R. H.; Roach, E.; Popov, A. I. *J. Am. Chem. Soc*. **1970**, *92*, 4989.
(26) Haynes, D. H.; Pressman, B. C.; Kowalsky, A. *Biochemistry* **1971**, *10*, 852.
(27) Kintzinger, J. P.; Lehn, J. M. *J. Am. Chem. Soc*. **1974**, *96*, 3313.
(28) Cornélis, A.; Laszlo, P. *Biochemistry* **1979**, *18*, 2004.
(29) Deverell, C. *Prog. Nucl. Magn. Reson. Spectrosc*. **1969**, *4*, 235.
(30) Laszlo, P. *Angew. Chem., Int. Ed. Engl*. **1978**, 17, 254.
(31) Forsén, S.; Lindman, B. In *NMR and the Periodic Table*; Harris, R. K., Mann, B. E., Eds.; Academic Press: London, 1978; Chapter 6.
(32) Wehrli, F. W. *Annu. Rep. NMR Spectrosc*. **1979**, *9*, 125.
(33) (a) Detellier, C. In *NMR of Newly Accessible Nuclei*; Laszlo, P., Ed.; Academic Press: New York, 1983; Vol. 2, pp 105−151. (b) Detellier, C.; Graves, H. P.; Brière, K. M. In *Isotopes in the Physical and Biomedical Sciences*, Buncel, E., Jones, J. R., Eds.; Elsevier Science Publishers B. V.: Amsterdam, 1991; pp 159−211.
(34) Akitt, J. W. In *Multinuclear NMR*; Mason, J., Ed.; Plenum Press: New York, 1987; Chapter 7.
(35) Buchanan, G. W. *Prog. Nucl. Magn. Reson. Spectrosc*. **1999**, *34*, 327.
(36) Tabeta, R.; Aida, M.; Saitô, H. *Bull. Chem. Soc. Jpn*. **1986**, *59*, 1957.
(37) Ellaboudy, A.; Tinkham, M. L.; Van Eck, B.; Dye, J. L.; Smith, P. B. *J. Phys. Chem*. **1984**, *88*, 3852.
(38) Ellaboudy, A.; Dye, J. L. *J. Magn. Reson*. **1986**, *66*, 491.
(39) Kim, J.; Dye, J. L. *J. Phys. Chem*. **1990**, *94*, 5399.
(40) Mason, E.; Eick, H. A. *Acta Crystsllogr*. **1982**, *B38*, 1821.
(41) Bush, M. A.; Truter, M. R. *J. Chem. Soc., Perkin Trans. 2* **1972**, 341.
(42) Dobler, M.; Dunitz, J. D.; Seiler, P. *Acta Crystallogr*. **1974**, *B30*, 2741.
(43) Bush, M. A.; Truter, M. R. *J. Chem. Soc. B* **1971**, 1440.
(44) Hughes, D. L. *J. Chem. Soc., Dalton Trans.* **1975**, 2374.
(45) Mathieu, F.; Metz, B.; Moras, D.; Weiss, R. *J. Am. Chem. Soc*. **1978**, *100*, 4412.
(46) (a) Metz, B.; Moras, D.; Weiss, R. *Chem. Commun*. **1971**, 444. (b) Moras, D.; Weiss, R. *Acta Crystallogr*. **1973**, *B29*, 396.
(47) Harris, R. K.; Nesbitt, G. J. *J. Magn. Reson*. **1988**, *78*, 245.
(48) Amoureux, J.-P.; Fernandez, C.; Steuernagel, S. *J. Magn. Reson., Ser. A* **1996**, *123*, 116.
(49) States, D. J.; Haberkorn, R. A.; Ruben, D. J. *J. Magn. Reson*. **1982**, *48*, 286.
(50) Moras, D.; Metz, B.; Herceg, M.; Weiss, R. *Bull. Soc. Chim. Fr*. **1972**, 551.
(51) Tehan, F. J.; Barnett, B. L.; Dye, J. L. *J. Am. Chem. Soc*. **1974**, *96*, 7203.
(52) Ward, D. L.; Wei, K. T.; Hoogerheide, J. G.; Popov, A. I. *Acta Crystallogr*. **1978**, *B34*, 110.
(53) Chiang, C. C.; Paul, I. C. *Science* **1977**, *196*, 1441.
(54) Laves, K. N.; Dobler, M. *Helv. Chim. Acta* **1975**, *58*, 432.
(55) Saitô, H.; Tabeta, R. *Bull. Chem. Soc. Jpn*. **1987**, *60*, 61.
(56) Dobler, M.; Phizackerley, R. P. *Helv. Chim. Acta* **1974**, *57*, 664.
(57) Wu, G.; Yamada, K. *Chem. Phys. Lett*. **1999**, *313*, 519.
(58) McManus, J.; Kemp-Harper, R.; Wimperis, S. *Chem. Phys. Lett*. **1999**, *311*, 292.
(59) Wi, S.; Frydman, L. *J. Chem. Phys*. **2000**, *112*, 3248.
(60) (a) Sagnowski, S. F.; Ogar, J. *Phys. Status Solidi* **1981**, *B107*, K125. (b) Sagnowski, S. F.; Sulek, Z.; Stachura, M.; Ogar, J. *Z. Phys*. **1982**, *B46*, 123.
(61) (a) Lutz, O. *Z. Naturforsch*. **1968**, *23a*, 1202. (b) Beckman, A.; Boklen, K. D.; Elke, D. *Z. Phys.* **1974**, *270*, 173.
(62) Ikenberry, D.; Das, T. P. *J. Chem. Phys*. **1965**, *43*, 2199. (b) **1966**, *45*, 1361.
(63) Deverell, C. *Mol. Phys*. **1969**, *16*, 491.
(64) Halliday, J. D.; Richards, R. E.; Sharp, R. R. *Proc. R. Soc. London* **1969**, *313A*, 45.
(65) de Dios, A. C.; Walling, A.; Cameron, I.; Ratcliffe, C. I.; Ripmeester, J. A. *J. Phys. Chem. A* **2000**, *104*, 908.
(66) Tossell, J. A. In *Modeling NMR Chemical Shifts: Gaining Insights into Structures and Environment*, Facelli, J. C., de Dios, A. C., Eds.; ACS Symposium Series 732; American Chemical Society: Washington, DC, 1999; pp 304−319.
(67) Brown, I. D.; Altermatt, D. *Acta Crystallogr*. **1985**, *B41*, 244.
(68) Wong, A.; Sham, S.; Wang, S.; Wu, G. *Can. J. Chem*. **2000**, *78*, 975.
(69) Wong, A.; Wu, G. Unpublished results, 2000.
(70) Bloor, E. G.; Kidd, R. G. *Can. J. Chem*. **1968**, *46*, 3425.
(71) Erlich, R. H.; Roach, E.; Popov, A. I. *J. Am. Chem. Soc*. **1970**, *92*, 4989.
(72) Gutmann, V.; Wychera, W. *Inorg. Nucl. Chem. Lett*. **1966**, *2*, 257.
(73) (a) Ramsey, N. F. *Phys. Rev*. **1950**, *78*, 699. (b) **1951**, *83*, 540. (c) **1952**, *86*, 243.
(74) Karplus, M.; Pople, J. A. *J. Chem. Phys*. **1963**, *38*, 2803.
(75) Jameson, C. J.; Gutowsky, H. S. *J. Chem. Phys*. **1964**, *40*, 1714.
(76) Pople, J. A. *Mol. Phys*. **1964**, *7*, 301.